GRAVITATIONAL LENSING

LECTURE 25

Docente: Massimo Meneghetti
AA 2015-2016

SUBHALOS/SUBSTRUCTURES AS A PROBE OF DM

- probing the mass function of DM sub-halos may be particularly useful to test scenarios such as WDM
- but also to test SIDM!
- Important thing to bear in mind: the typical scale of the ER in the case of a dwarf satellite is few mas (e.g. WDM)
- SL by galaxies in clusters may help to constrain the sub-halos on larger scales

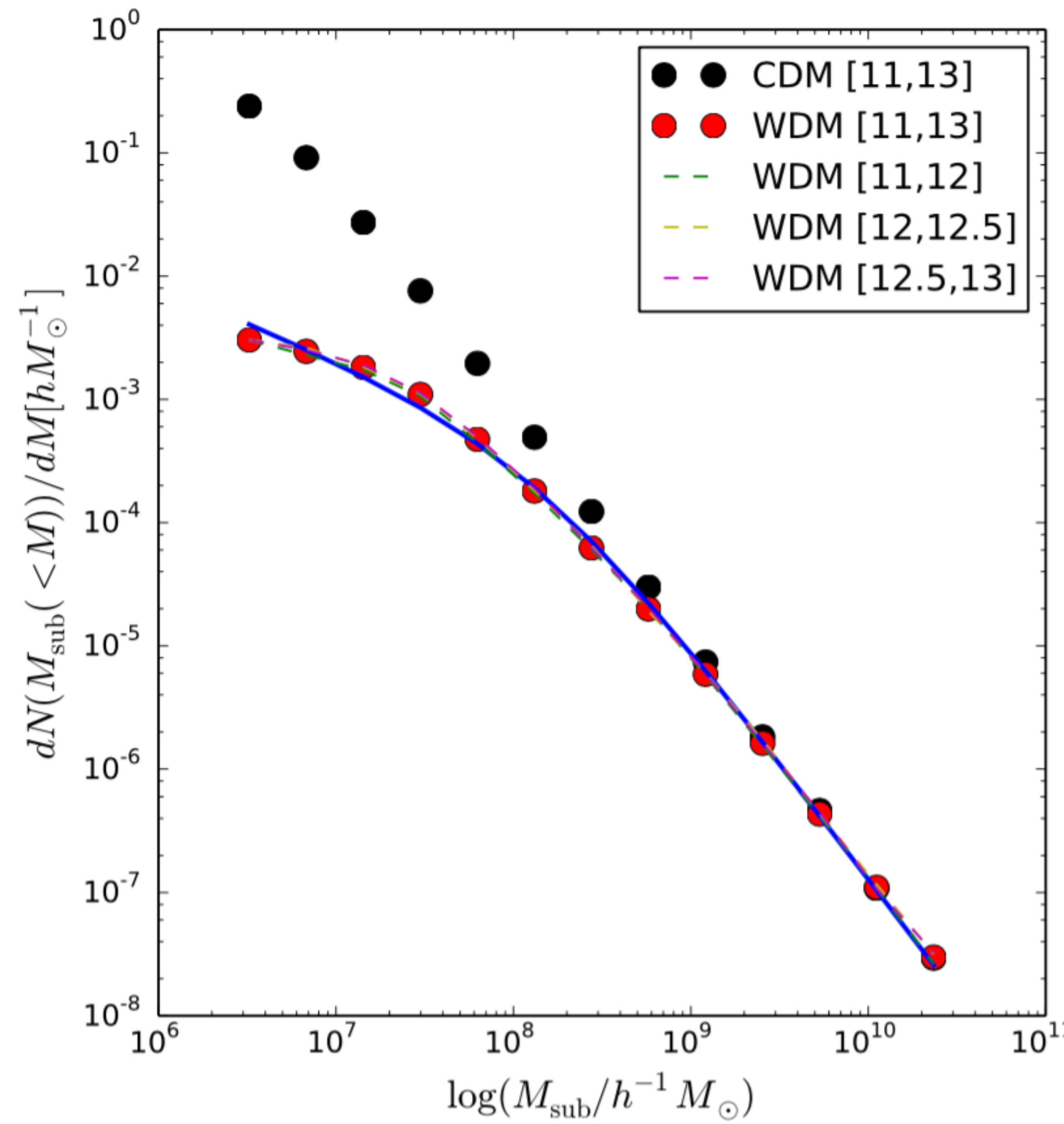

SUBSTRUCTURES FROM SL: FLUX ANOMALIES

- substructures detectable as magnification anomalies (second derivatives of the potential) of point like sources
  - easy to model
  - sensitive to wide range of masses
  - some theoretically established relations for cusp and fold images

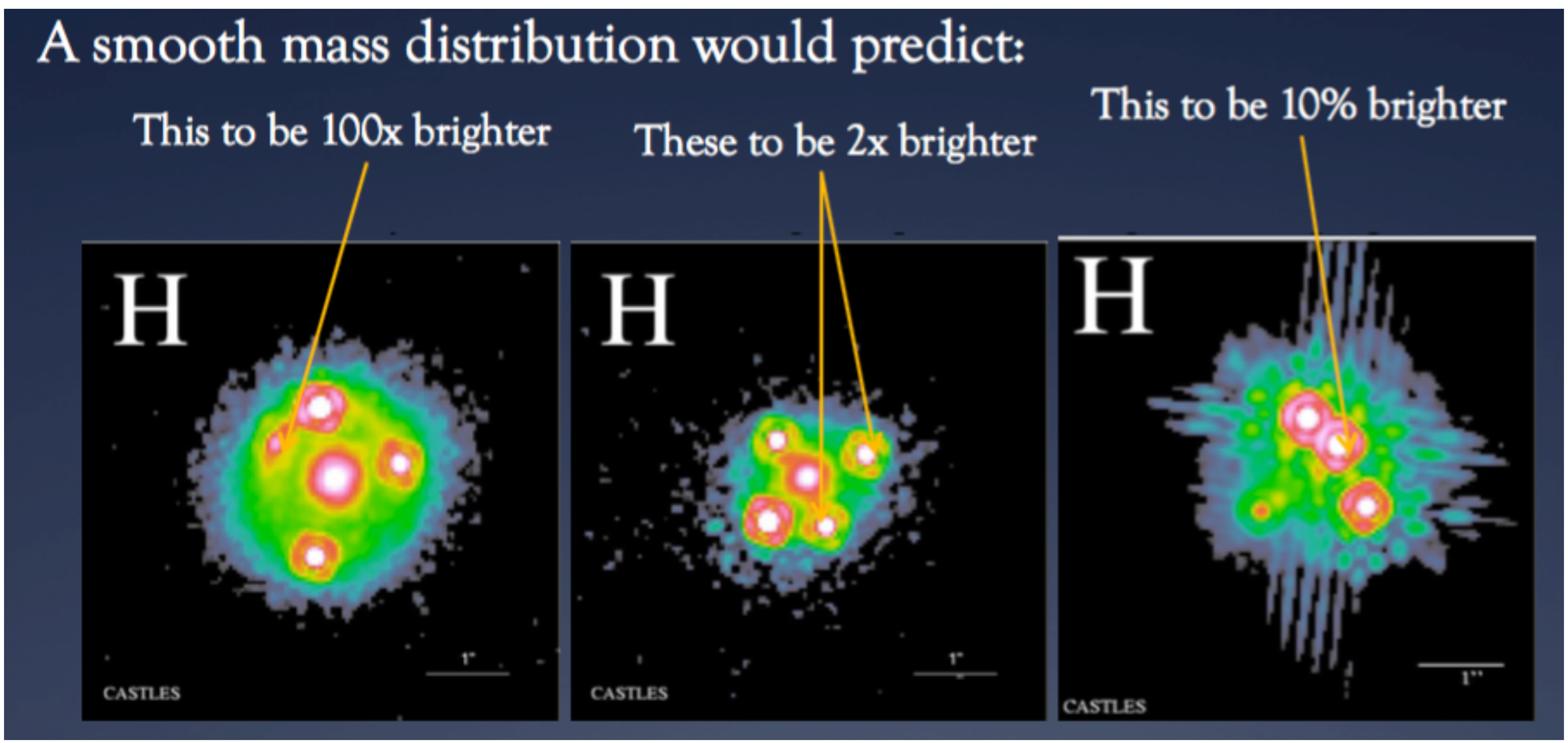

SUBSTRUCTURES FROM SL: FLUX ANOMALIES

detected in 7 radio lenses

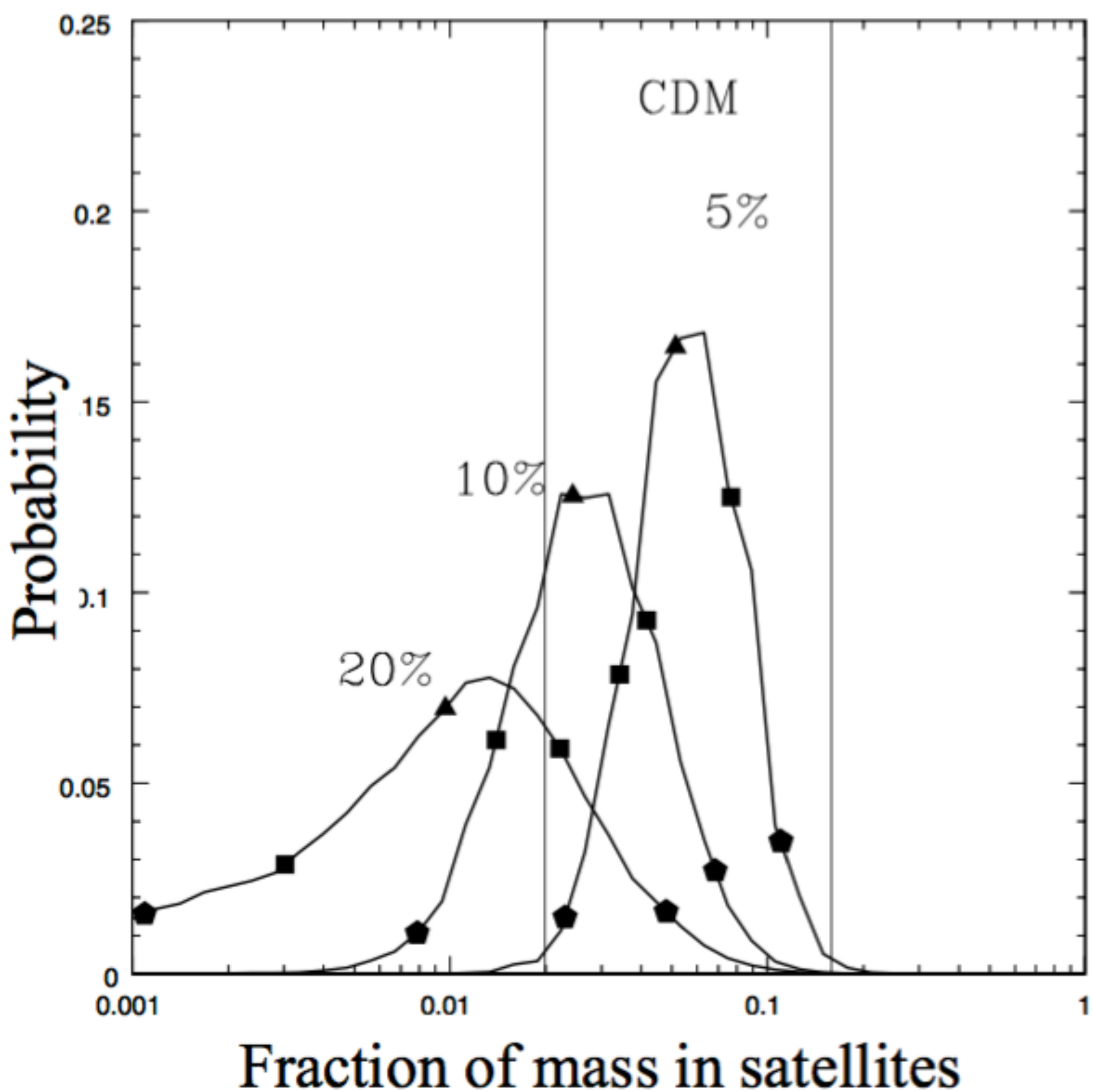

Dalal & Kochanek (2002): flux anomalies consistent with a fraction of mass in sub halos within the ER f~0.02

This is consistent with simulations in the framework of CDM

SUBSTRUCTURES FROM SL: GRAVITATIONAL IMAGING

- substructures are detected as surface brightness anomalies (i.e. astrometric anomalies, first derivatives of the potential)
  - sensitive to larger masses
  - becoming more efficient thanks to the achievement for higher resolutions: ALMA, adaptive optics, GVLBI (astrometric perturbations of the order of $\sim$10 mas)

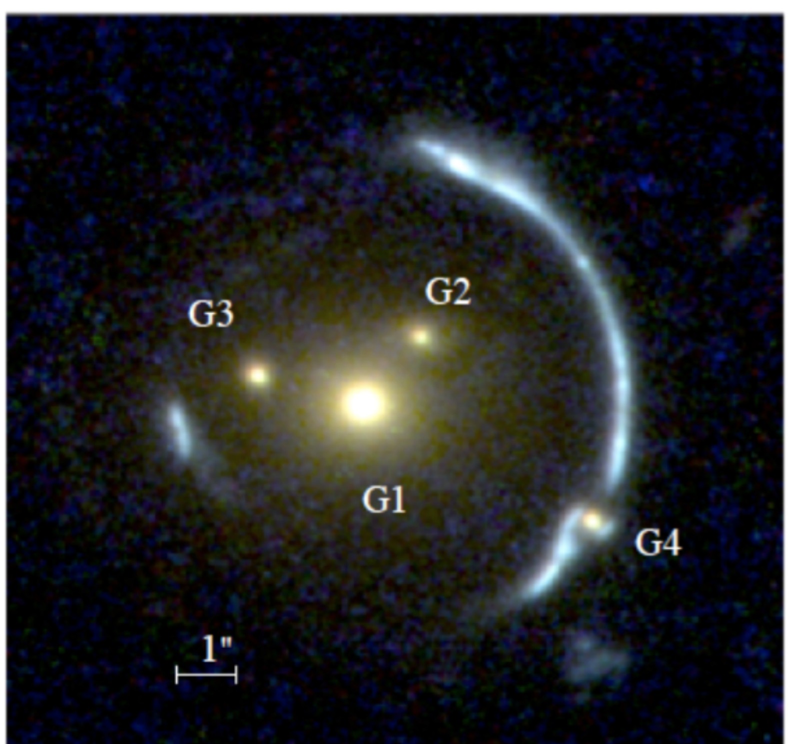

E.g. Vegetti et al. 2014

$$\psi(\mathbf{x},\eta)_{tot} = \psi(\mathbf{x},\eta) + \delta\psi(\mathbf{x})$$

$\psi(\mathbf{x},\eta)$ Smooth analytic power-law model

$\delta\psi(\mathbf{x})$ pixellated potential correction

SUBSTRUCTURES FROM SL: GRAVITATIONAL IMAGING

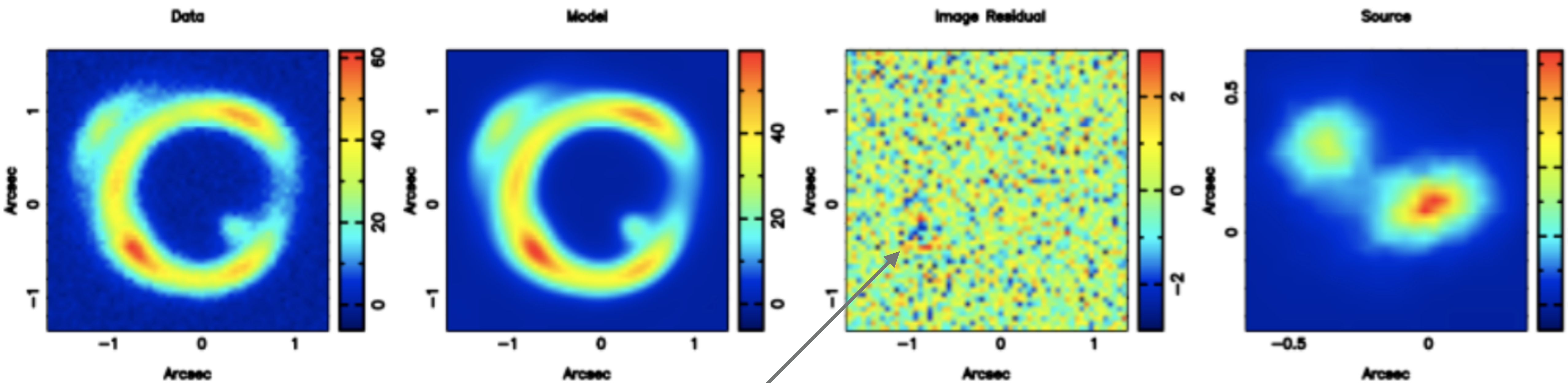

Substructures detected as corrections to a smooth potential

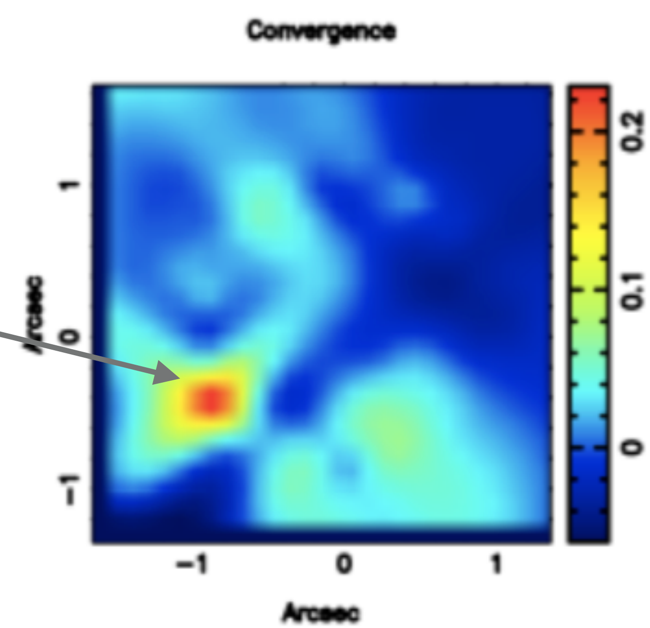

Density corrections

Issue: in addition to the usual modeling uncertainties, need to disentangle the structure in the potential from those in the sources

SUBSTRUCTURES FROM SL: GRAVITATIONAL IMAGING

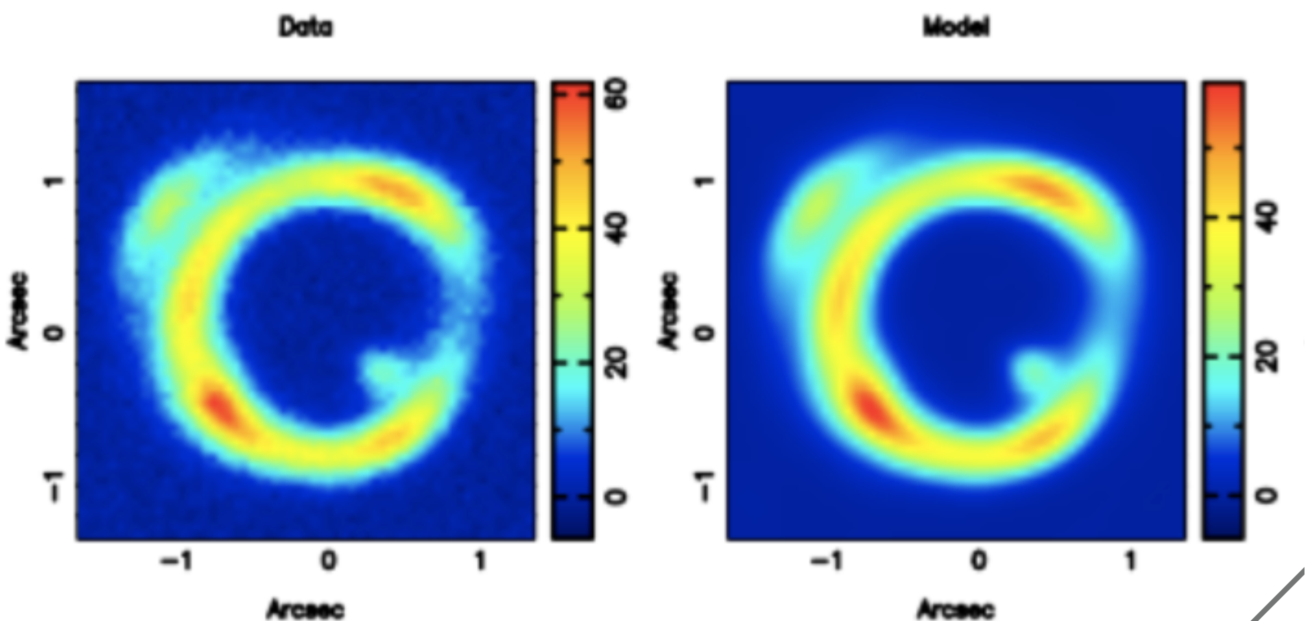

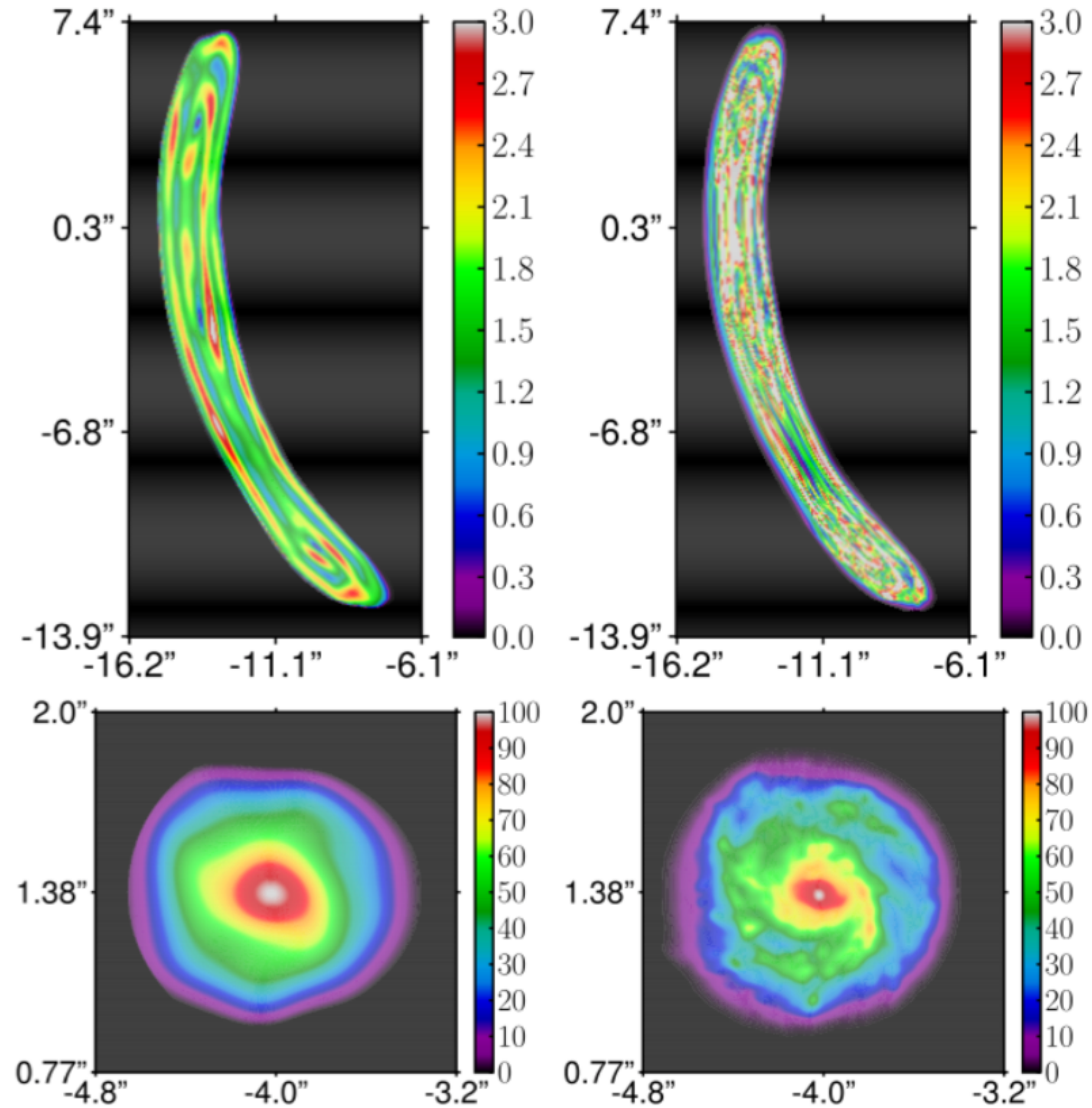

Substructures detected as corrections to a smooth potential

Issue: in addition to the usual modeling uncertainties, need to disentangle the structure in the potential from those in the sources

SUBSTRUCTURES FROM SL: GRAVITATIONAL IMAGING

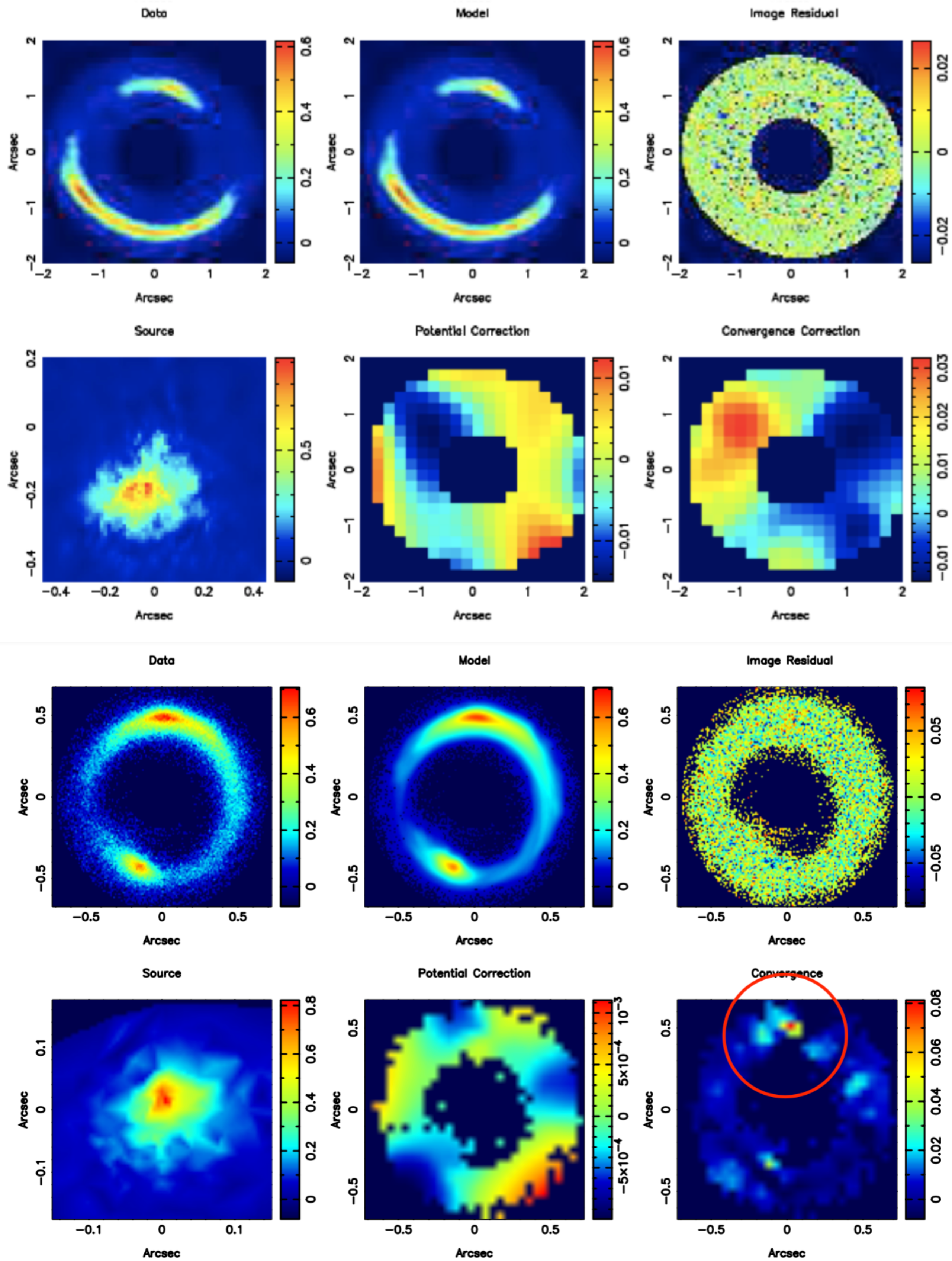

Vegetti et al. 2010, 2012, 2014:

substructures detected at high significance level (>10σ)

$$M_{\rm sub} \sim 2 - 40 \times 10^8 M_\odot$$

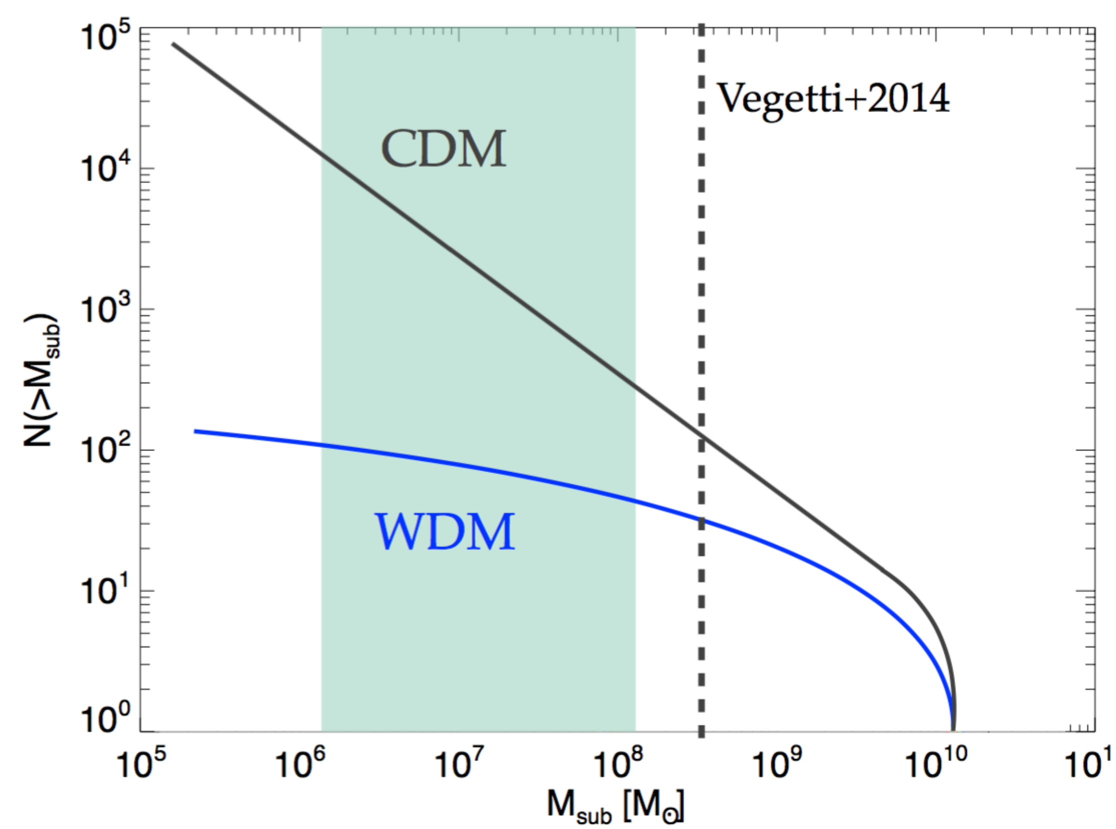

THE FRONTIER FIELDS INITIATIVE

(P.I. MATT MOUNTAIN, JENNIFER LOTZ)

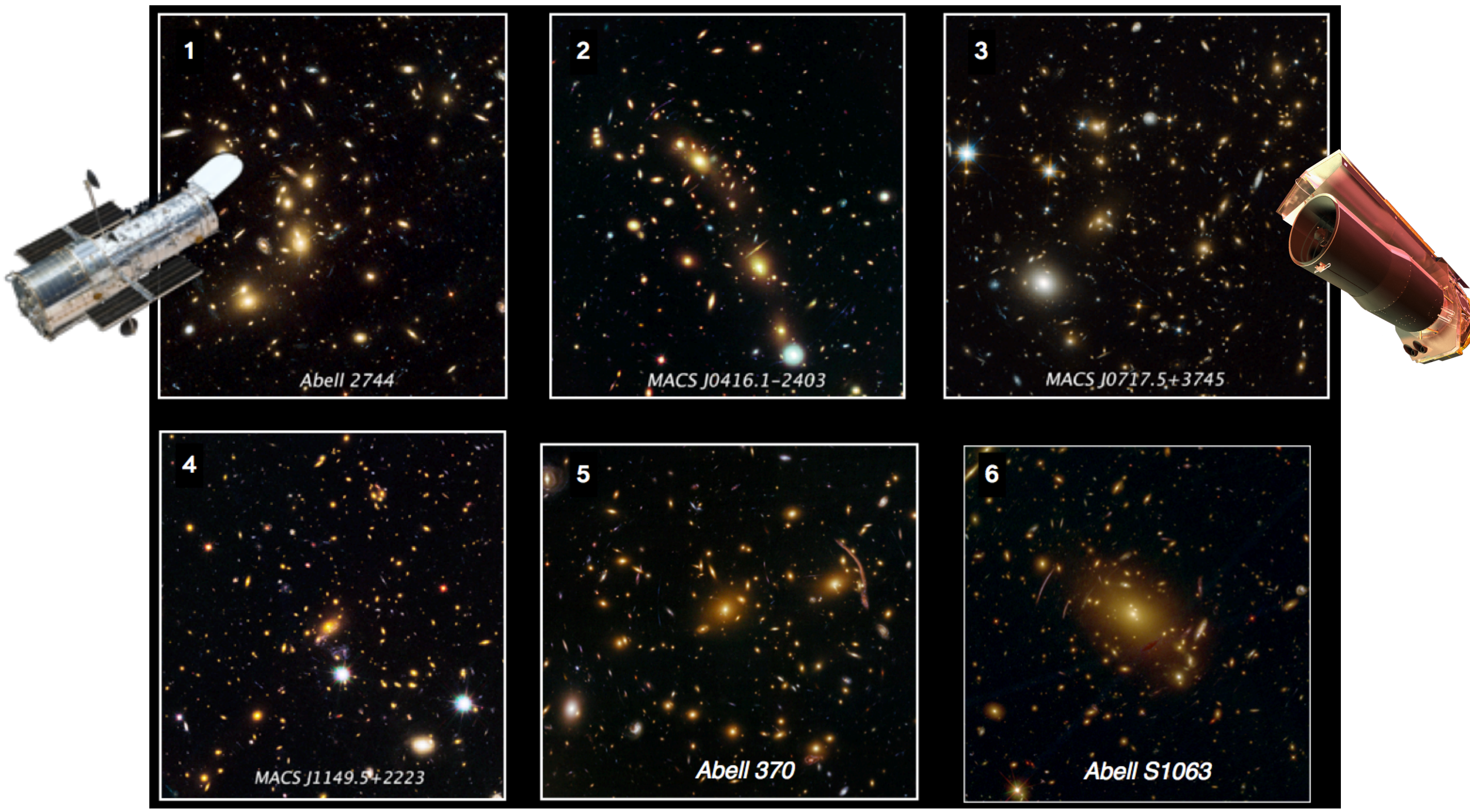

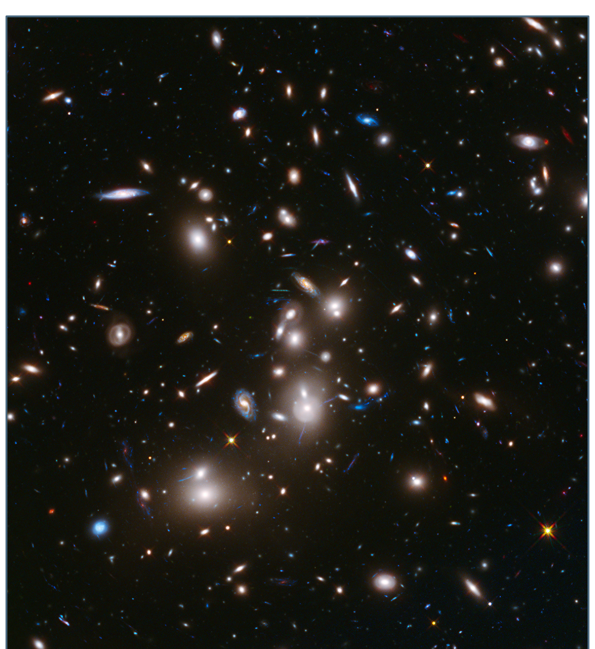

- 6 lensed + 6 parallel fields
- 840 Hubble orbits +1000 Spitzer hrs directors' discretionary time
- Cycles 21, 22, 23
- Strongest lenses with low zodiacal bkg, galactic extinction, observable with ALMA
- Complemented by Chandra, Subaru, VLT Hawk-I, Gemini, spectra from Keck, Photo-z

ACS: (70 orbits per position)			WFC3/IR: (70 orbits per position)		
Filter	Orbits	AB_mag	Filter	Orbits	AB_mag
F435W	18	28.8	F105W	24	28.9
F606W	10	28.8	F125W	12	28.6
F814W	42	29.1	F140W	10	28.6
			F160W	24	28.7

Cluster Name	z	Cluster		Parallel Field		HST FOV	Regions File
		RA	Dec	RA	Dec		
Year 1:							
Abell 2744	0.308	00:14:21.2	-30:23:50.1	00:13:53.6	-30:22:54.3		regions
MACSJ0416.1-2403	0.396	04:16:08.9	-24:04:28.7	04:16:33.1	-24:06:48.7		regions
Year 2:							
MACSJ0717.5+3745	0.545	07:17:34.0	+37:44:49.0	07:17:17.0	+37:49:47.3		regions
MACSJ1149.5+2223	0.543	11:49:36.3	+22:23:58.1	11:49:40.5	+22:18:02.3		regions
Year 3:							
Abell S1063 (RXCJ2248.7-4431)	0.348	22:48:44.4	-44:31:48.5	22:49:17.7	-44:32:43.8		regions
Abell 370	0.375	02:39:52.9	-01:34:36.5	02:40:13.4	-01:37:32.8		regions

Frontier Fields Visit Status Page

How To Use This Page

Observed Scheduling Long Range Planning High Level Science Products (full-depth mosaics)

		2013			2014												2015												2016						
	Progress	Oct	Nov	Dec	Jan	Feb	Mar	Apr	May	Jun	Jul	Aug	Sep	Oct	Nov	Dec	Jan	Feb	Mar	Apr	May	Jun	Jul	Aug	Sep	Oct	Nov	Dec	Jan	Feb	Mar	Apr	May	Jun	Jul
ABELL-2744	100.0%	WFC3	WFC3						ACS	ACS	ACS																								
ABELL-2744-HFFPAR	100.0%	ACS	ACS						WFC3	WFC3	WFC3																								
MACSJ0416.1-2403	100.0%				ACS	ACS					WFC3	WFC3	WFC3																						
MACSJ0416.1-2403-HFFPAR	100.0%				WFC3	WFC3					ACS	ACS	ACS																						
MACSJ0717.5+3745	50.0%	ACS											ACS	ACS	ACS			WFC3	WFC3	WFC3															
MACSJ0717.5+3745-HFFPAR	50.0%	WFC3											WFC3	WFC3	WFC3			ACS	ACS	ACS															
MACSJ1149.5+2223	51.4%		WFC3					ACS							WFC3	WFC3	WFC3			ACS	ACS	ACS													
MACSJ1149.5+2223-HFFPAR	51.4%		ACS					WFC3							ACS	ACS	ACS			WFC3	WFC3	WFC3													
ABELL-S1063	1.4%													ACS											ACS	ACS	ACS	ACS				WFC3	WFC3	WFC3	WFC3
ABELL-S1063-HFFPAR	1.4%													WFC3											WFC3	WFC3	WFC3	WFC3				ACS	ACS	ACS	ACS

HST Frontier Fields Data Overview
HST Frontier Fields Archive Data Products Page

MAST High Level Data Pages:

- ABELL-2744 + Parallel Field
- MACSJ0416.1-2403 + Parallel Field
- MACSJ0717.5+3745 + Parallel Field
- MACSJ1149.5+2223 + Parallel Field
- ABELL-S1063 + Parallel Field

Last updated: 2015-02-04T19:01:21.163230

MACSJ0416 **1. Before HFF ...**

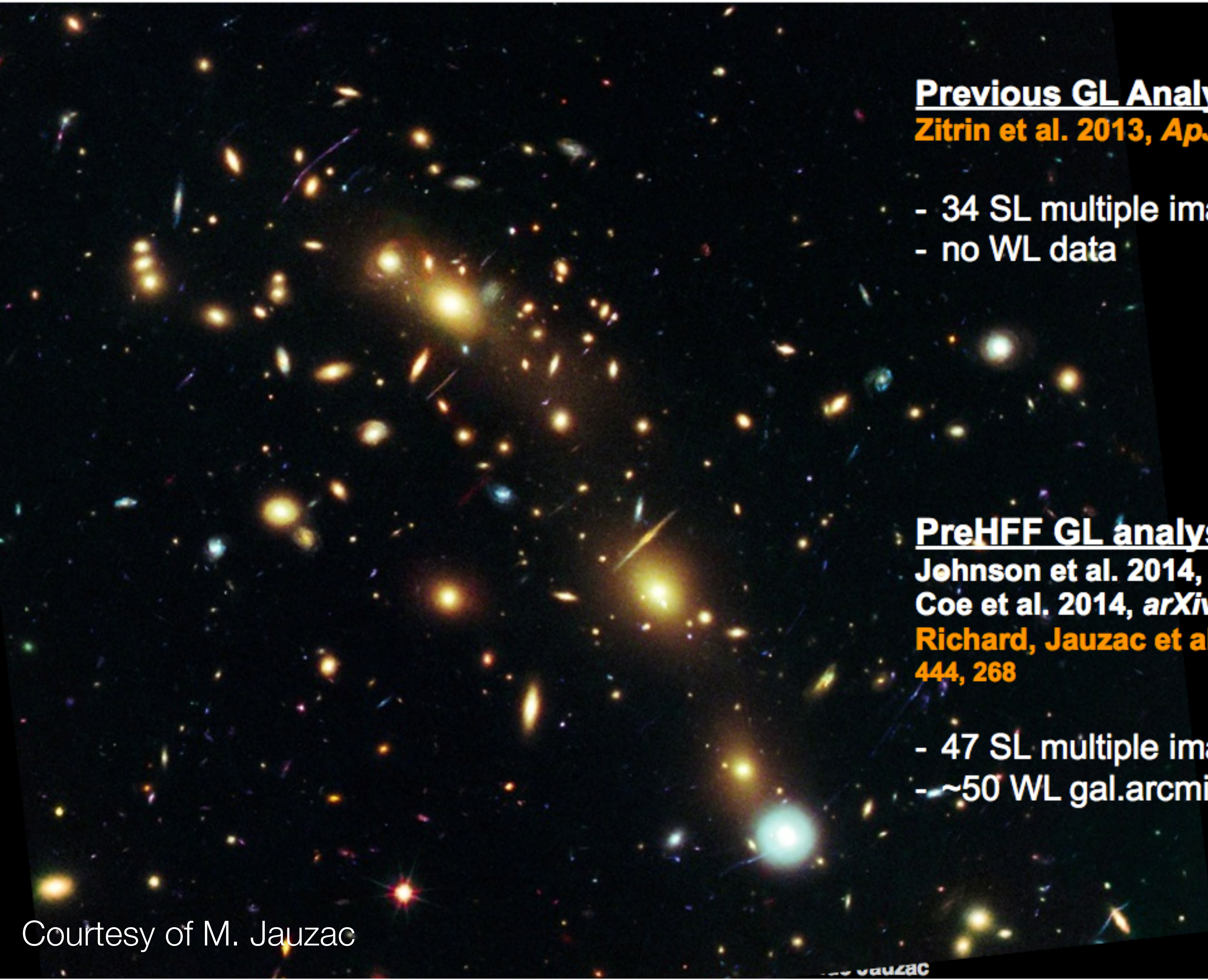

Previous GL Analysis :
Zitrin et al. 2013, *ApJ, 762, 30*

- 34 SL multiple images
- no WL data

PreHFF GL analysis :
Johnson et al. 2014, *arXiv 1405.0222*
Coe et al. 2014, *arXiv 1405.0011*
Richard, Jauzac et al. 2014, MNRAS, 444, 268

- 47 SL multiple images
- ~50 WL gal.arcmin^{-2}

Courtesy of M. Jauzac

1. … After HFF !!!

Jauzac et al. 2014a, *MNRAS, 443, 1549*
Jauzac et al. 2014b, *arXiv, 1406.3011*

194 SL multiple images

~100 WL gal.arcmin^{-2}

MACSJ0416 :
the MOST constrained galaxy cluster to date !!!

STRONG GALAXY-GALAXY LENSING IN CLUSTERS

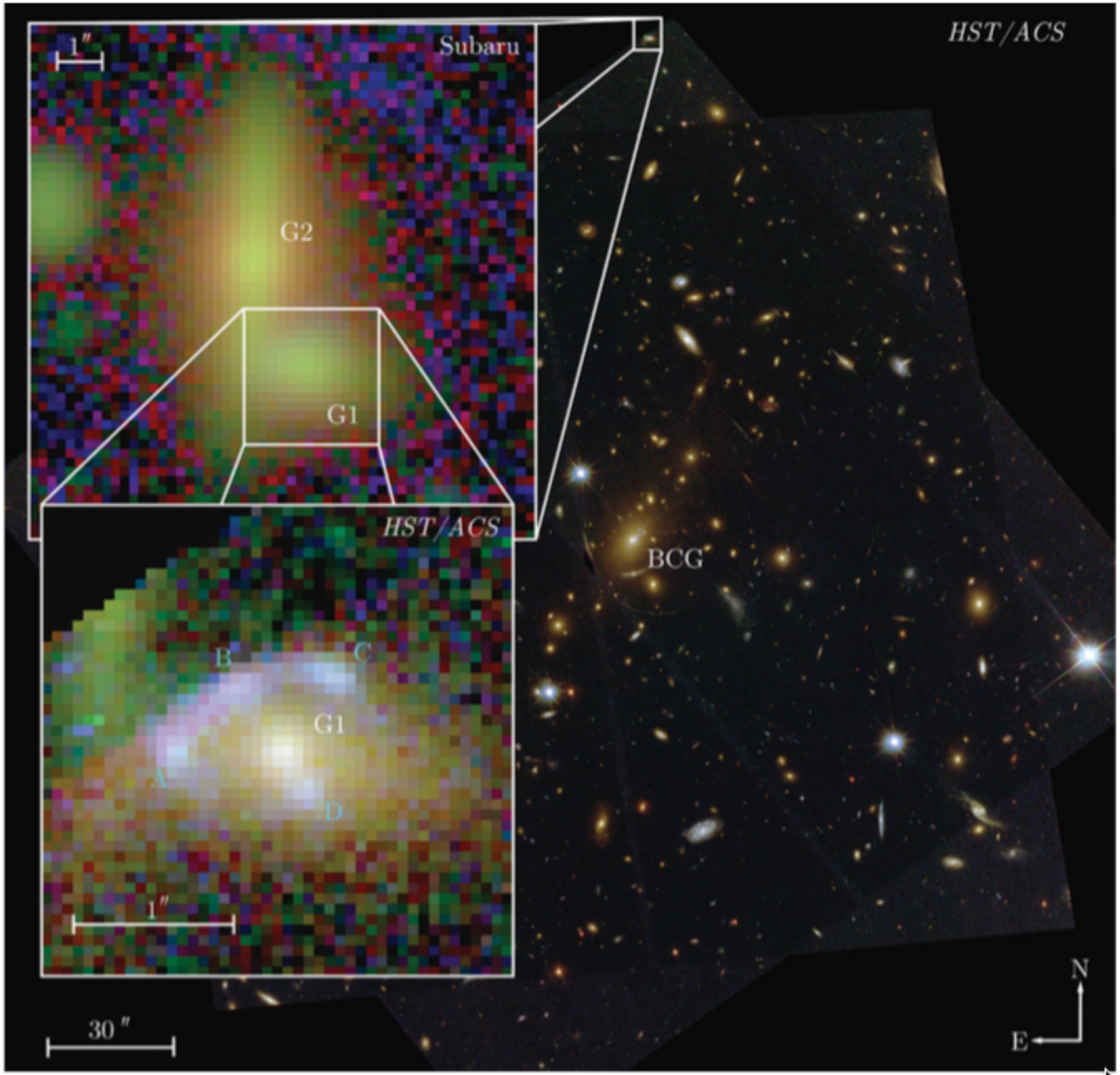

Parry et al. 2016

FRONTIER FIELDS: AN EXCESS OF DM SUB HALOS COMPARED TO SIMULATIONS?

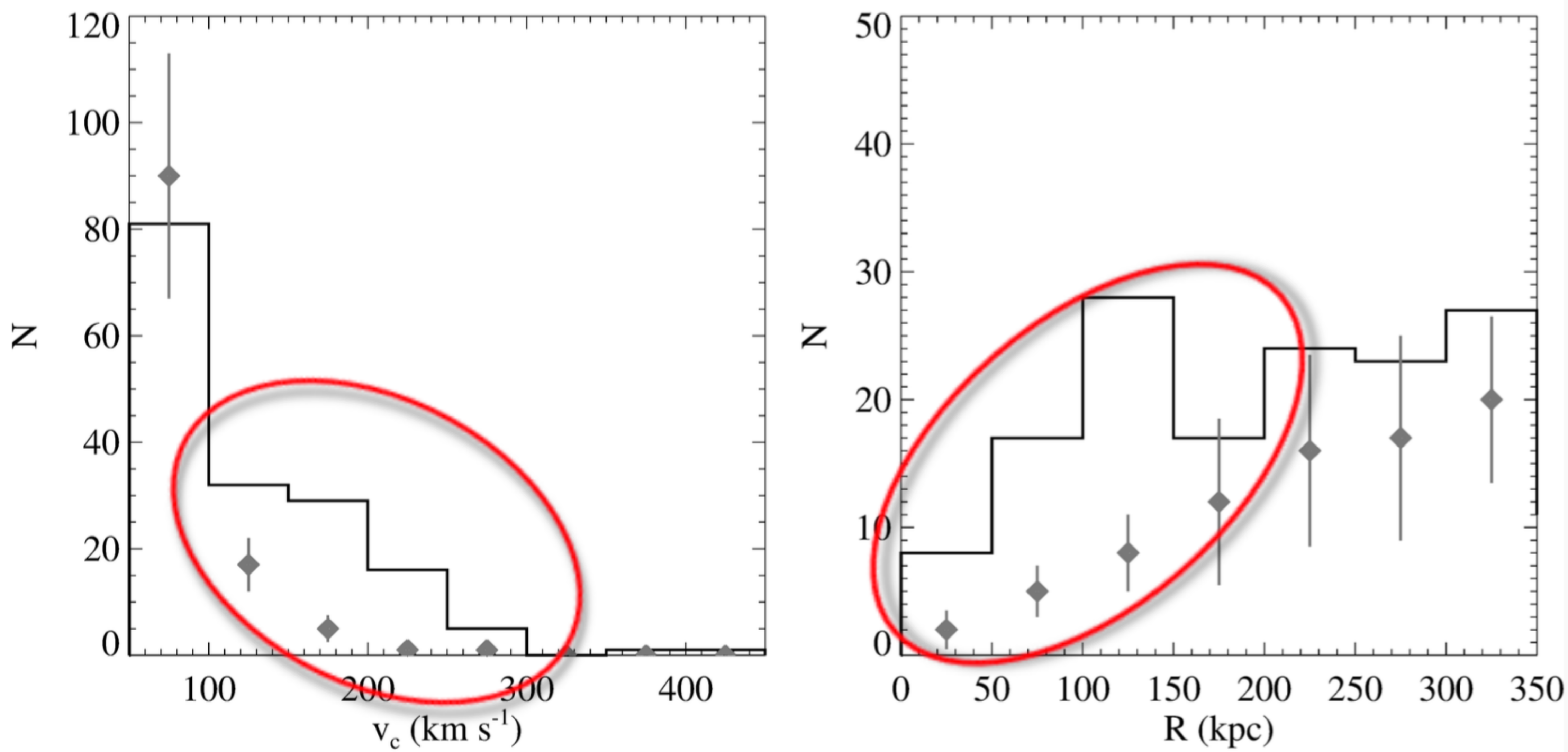

MACS J0416 - Grillo+15a

COSMOGRAPHY WITH TIME DELAYS

Treu & Marshall, 2016

Time delay distance $\propto \dfrac{1}{H_0}$

Distances encode information on additional cosmological parameters!

$$\tau(\boldsymbol{\theta}) = \frac{D_{\Delta t}}{c} \cdot \Phi(\boldsymbol{\theta}, \boldsymbol{\beta}),$$

$$\text{where } \Phi(\boldsymbol{\theta}) = \frac{1}{2}(\boldsymbol{\theta} - \boldsymbol{\beta})^2 - \psi(\boldsymbol{\theta}).$$

Obtain from the lens mass model

- Needed ingredients:
  - Time delays
  - lens mass model

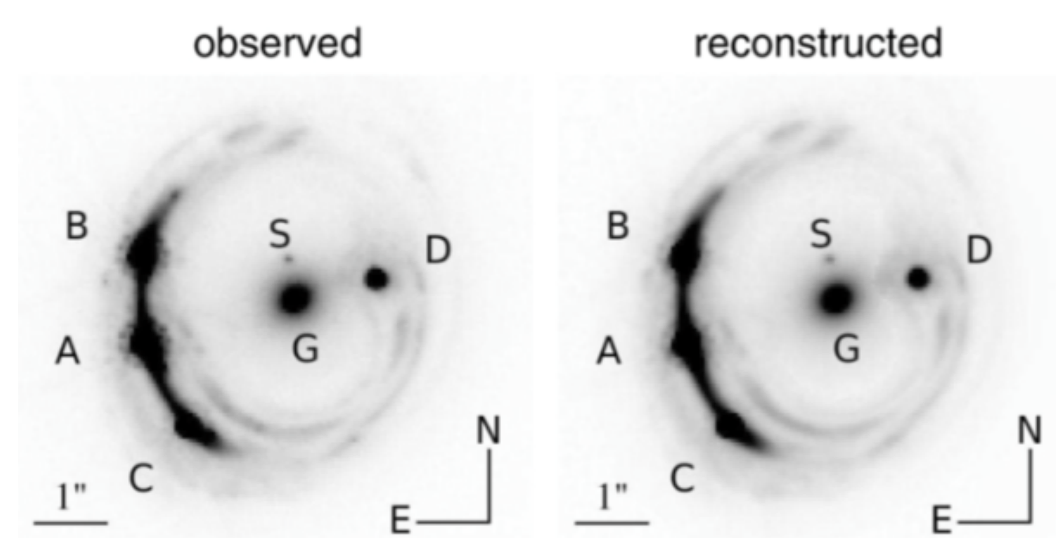

THE HUBBLE CONSTANT FROM TIME DELAYS

ON THE POSSIBILITY OF DETERMINING HUBBLE'S PARAMETER AND THE MASSES OF GALAXIES FROM THE GRAVITATIONAL LENS EFFECT*

Sjur Refsdal

(Communicated by H. Bondi)

(Received 1964 January 27)

Summary

The gravitational lens effect is applied to a supernova lying far behind and close to the line of sight through a distant galaxy. The light from the supernova may follow two different paths to the observer, and the difference Δt in the time of light travel for these two paths can amount to a couple of months or more, and may be measurable. It is shown that Hubble's parameter and the mass of the galaxy can be expressed by Δt, the red-shifts of the supernova and the galaxy, the luminosities of the supernova "images" and the angle between them. The possibility of observing the phenomenon is discussed.

---

1. *Introduction.*—In 1937 Zwicky suggested that a galaxy, due to the gravitational deflection of light, may act as a gravitational lens. He considered the case of a galaxy *A* lying far behind and close to the line of sight through a distant galaxy *B*. If the line of sight through the centre of *B* goes through *A*, the "image" of *A* will be a ring around *B*, otherwise two separated "images" appear, on opposite sides of *B*. The phenomenon has later been discussed by Zwicky (1957) and Klimov (1963), and they both conclude that the possibility of observing the phenomenon should be good. In the present paper the case of a supernova

TABLE 2

Hubble Constant from Each Lens System

Lens Name	h (1 σ Range)
B0218+357	0.21 (. . .)
HE 0435−1223	1.02 (0.70–1.39)
RX J0911+0551	0.96 (0.75–1.21)
SBS 0909+532	0.84 (0.47–)
FBQ 0951+2635	0.67 (0.56–0.81)
Q0957+561	0.99 (0.82–1.17)
HE 1104−1805	1.04 (0.92–1.22)
PG 1115+080	0.66 (0.49–0.84)
RX J1131−1231	0.79 (0.59–1.03)
B1422+231	0.16 (–0.36)
SBS 1520+530	0.53 (0.46–0.61)
B1600+434	0.65 (0.54–0.77)
B1608+656	0.89 (0.77–1.20)
SDSS J1650+4251	0.53 (0.44–0.63)
PKS 1830−211	0.88 (0.58–)
HE 2149−2745	0.69 (0.57–0.82)
All	0.70 (0.68–0.73)

Note.—The Hubble constant and its error are estimated from the effective χ^2.

Oguri et al. 2007

CURRENT MEASUREMENTS OF TIME DELAYS

Enormous progress in the quality of the light curves since the first measurements thanks to dedicated networks of telescopes. For example: the COSMOGRAIL project measured time delays with precision <4% for 5 lenses

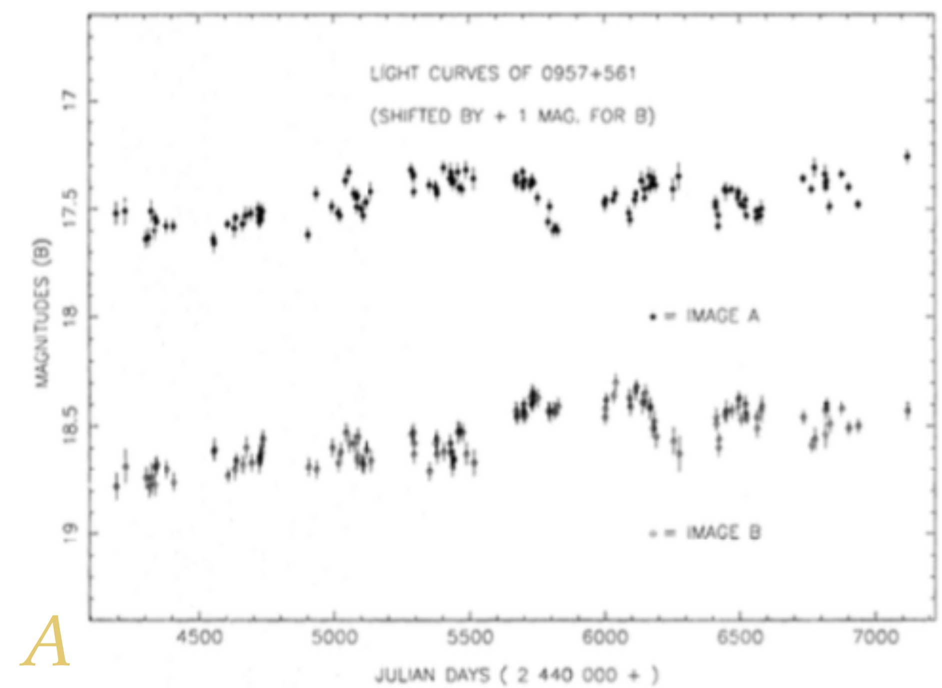

0957+561

Vanderriest et al. 1989

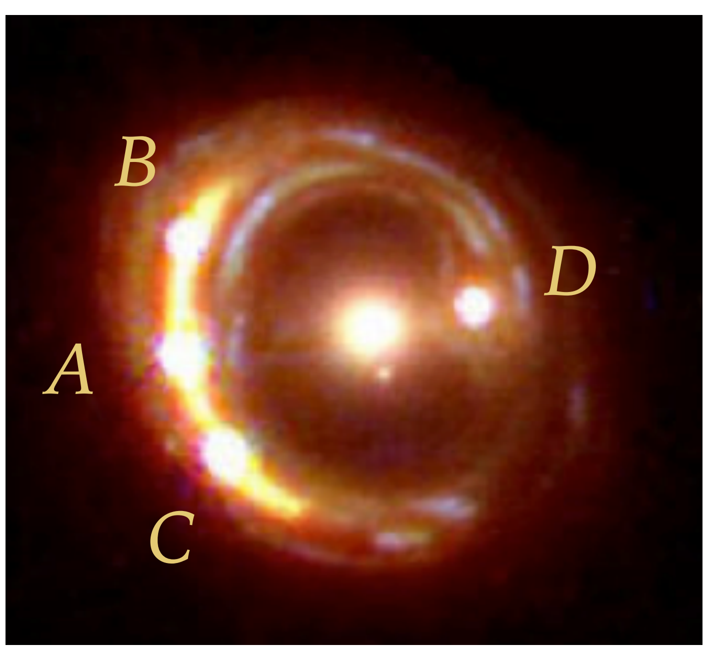

RXJ1131

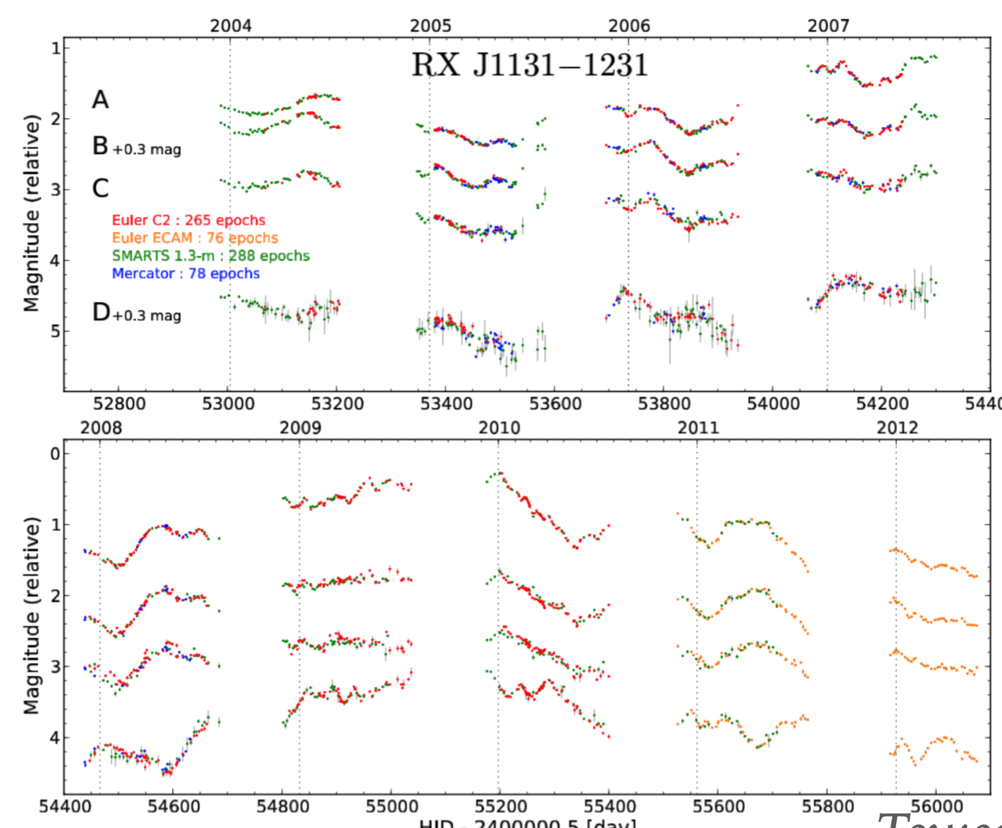

Tewes et al. 2013b

CURRENT CONSTRAINTS ON COSMOLOGY FROM TIME DELAYS

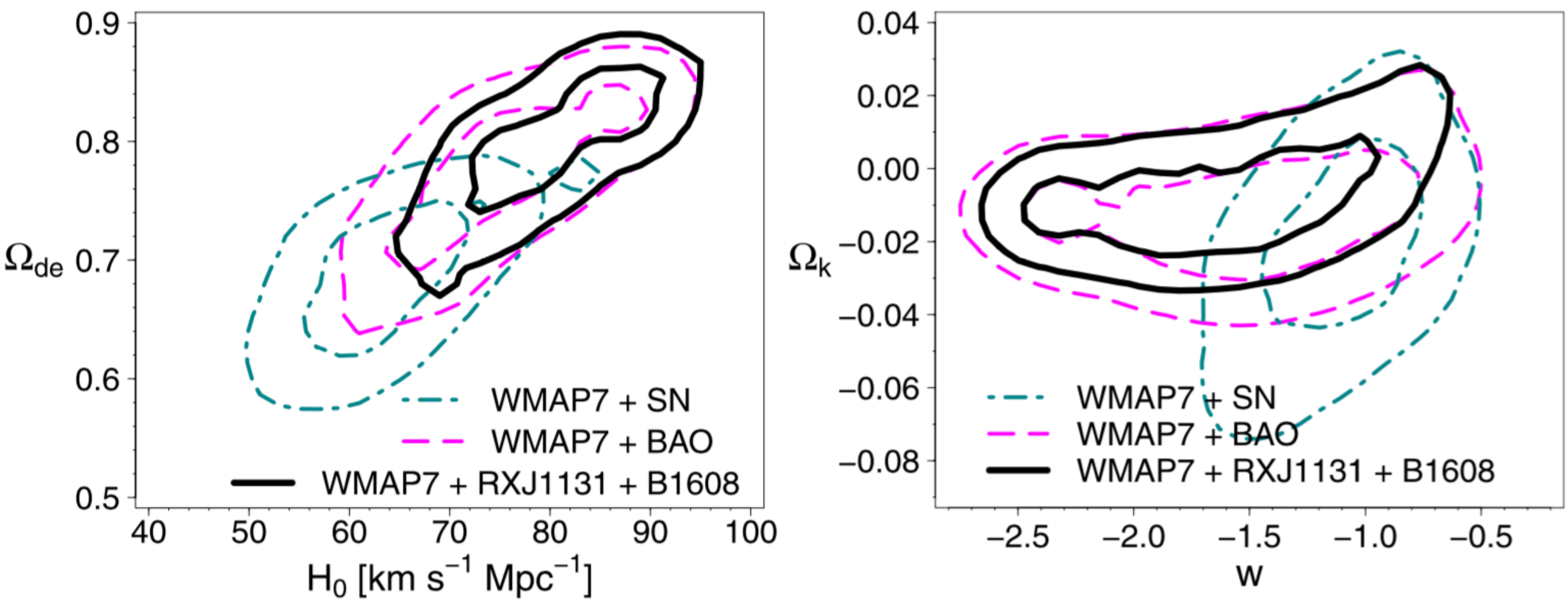

Suyu et al. 2013

Results are going to improve by means of the combination of many lenses (e.g. LSST)

COSMOGRAPHY WITH SOURCES AT MULTIPLE REDSHIFTS

- Even if time delay measurements are not available, the sensitivity to cosmology remains in the astrometric constraints
- With only one lensed source, the distance ratio is degenerate with the mass distribution
- With constraints from multiple sources, one can try to break the degeneracy by measuring the so called "family ratio"
- This technique could be used in the case of e.g. compound lenses, but also in galaxy clusters, where it is easier to observe lensing of many sources

$$\vec{\beta} = \vec{\theta} - \frac{D_{LS}}{D_S}\hat{\vec{\alpha}}(\vec{\theta})$$

depends on cosmology

depends on the mass distr.

$$\Xi_{S1,S2}(\vec{\pi}) = \frac{D_{LS,1}(\vec{\pi})D_{S,2}(\vec{\pi})}{D_{LS,2}(\vec{\pi})D_{S,1}(\vec{\pi})}$$

COSMOGRAPHY: GALAXY CLUSTERS

Mass model with 3 PIEMD potentials; 58 cluster galaxies
Bayesian optimization: 32 constraints, 21 free parameters;
RMS = 0.6 arcsec; 28 multiple images from 12 sources with
spec z, flat Universe prior

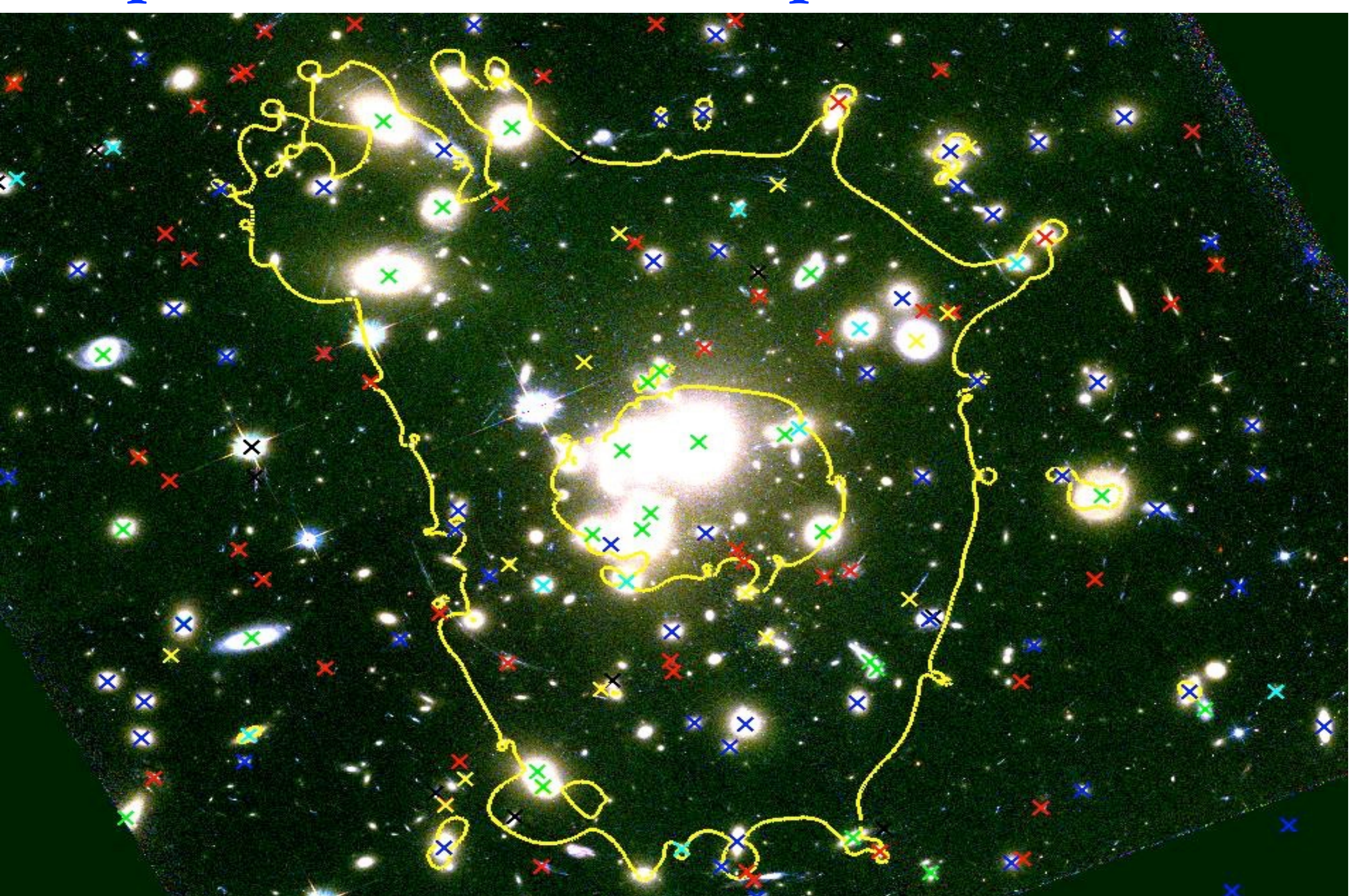

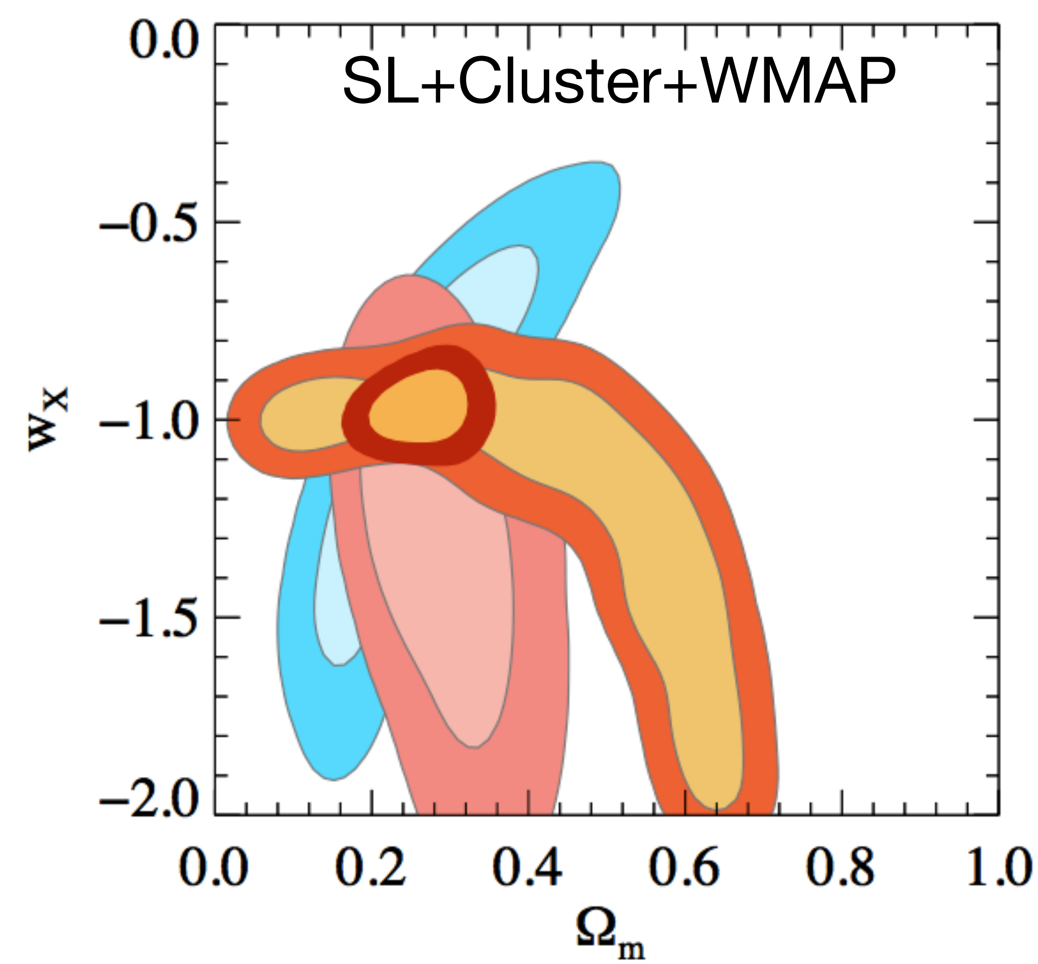

D'Aloisio & Natarajan 10; Jullo & Kneib 09: Jullo+ 10

COSMOGRAPHY: GALAXY CLUSTERS

Caminha et al. 2016

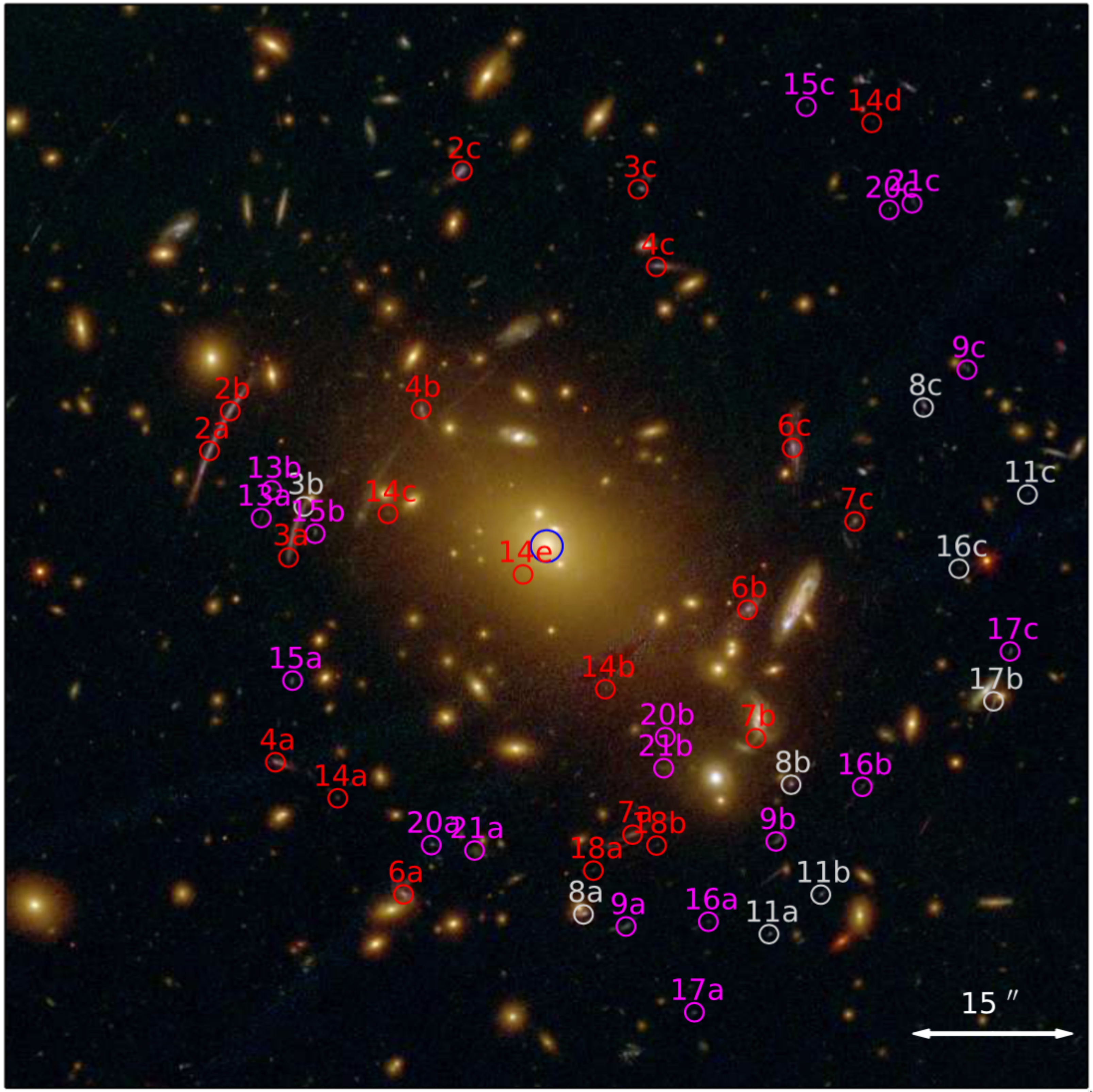

Abell S1063@z=0.348 is one of the FFs.

Spectroscopic follow-up with VIMOS and MUSE @VLT allowed to measure redshifts for 10 families of multiple images (z=1.035-6.111)+confirm the membership of many cluster galaxies.

Very accurate mass modeling, using only secured lensing constraints

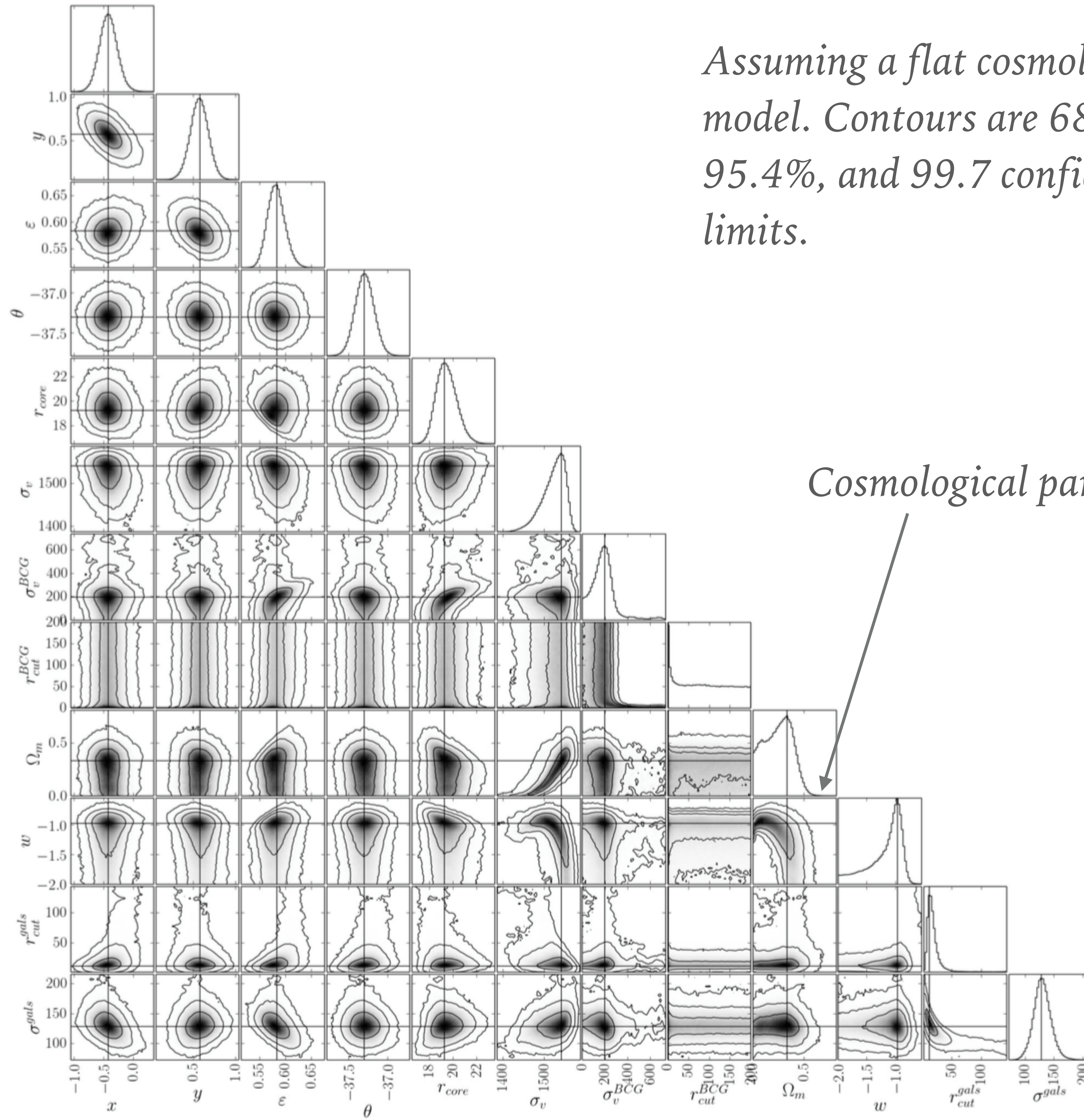

Assuming a flat cosmological model. Contours are 68%, 95.4%, and 99.7 confidence limits.